DENTAL MATERIALS 35 (2019) 1238–1253

Available online at www.sciencedirect.com

ScienceDirect

journal homepage: www.intl.elsevierhealth.com/journals/dema

Treated dentin matrix particles combined with dental follicle cell sheet stimulate periodontal regeneration

Hefeng Yang[a,b,1], *Jie Li*[c,1], *Yu Hu*[d], *Jingjing Sun*[b,e], *Weihua Guo*[b,e], *Hui Li*[b,e], *Jinglong Chen*[b,e], *Fangjun Huo*[b], *Weidong Tian*[b,e,**], *Song Li*[a,*]

[a] *Department of Dental Research, The Affiliated Stomatological Hospital of Kunming Medical University, Kunming, Yunnan 650500, PR China*

[b] *National Engineering Laboratory for Oral Regenerative Medicine, Sichuan University, Chengdu 610041, PR China*

[c] *Chongqing Key Laboratory of Oral Diseases and Biomedical Sciences, College of Stomatology, Chongqing Medical University, Chongqing 401147, PR China*

[d] *Department of Orthodontics, The Affiliated Stomatological Hospital of Kunming Medical University, Kunming, Yunnan 650031, PR China*

[e] *Department of Oral and Maxillofacial Surgery, West China Hospital of Stomatology, Sichuan University, Chengdu 610041, PR China*

ARTICLE INFO

Article history:
Received 15 February 2019
Received in revised form
14 May 2019
Accepted 16 May 2019

Keywords:
Periodontal regeneration
Dental follicle cell
Cell sheet engineering
Dentin matrix

ABSTRACT

Objective. Periodontal tissue engineering is an attractive approach for restoring periodontal-supporting structures and functions. However, complete periodontal regeneration has not been accomplished. Previous studies demonstrated the feasibility of using cell sheets and treated dentin matrix (TDM) to regenerate bio-roots.

Methods. In this study, we regenerated periodontal tissue using cell sheets combined with TDM particles (TDMPs). Human dental follicle cells (hDFCs) were isolated and characterized. Human dental follicle cells sheets (hDFCSs) and human TDMPs (hTDMP) were fabricated and characterized. The osteogenic effect of hTDMP was evaluated on human bone marrow stromal cells (hBMSCs) *in vitro* and a rat calvarial bone defect *in vivo*. Real-time PCR, western blotting, radiograph analysis, and histological analysis were performed to evaluate the periodontal induction capacity of hTDMP. One-wall periodontal intrabony defects were prepared to evaluate the periodontal regeneration capacity of TDMP/DFCSs on beagle dogs.

Results. The results showed that hDFCs were mesenchymal stem cells. hTDMP promoted the proliferation and osteogenic differentiation of hBMSCs. New bone formation was observed in the rat calvarial bone defect zone in both the hTDMP and hydroxyapatite/β-tricalcium phosphate groups. Periodontal-like tissues showed better regeneration in the canine TDMP + DFCS group than in the other groups.

* *Corresponding author at*: Department of Dental Research, The Affiliated Stomatological Hospital of Kunming Medical University, Kunming, Yunnan 650500, P.R. China.

** *Corresponding author at*: Department of Oral and Maxillofacial Surgery, West China School of Stomatology, Sichuan University, No. 14, 3rd Section, Renmin South Road, Chengdu 610041, PR China.

E-mail addresses: drtwd@sina.com (W. Tian), lisong59@sohu.com (S. Li).

[1] These authors contributed equally to this work.

https://doi.org/10.1016/j.dental.2019.05.016

Significance. These results demonstrate the potential of using TDMP/DFCSs in periodontal regeneration.

1. Introduction

Periodontitis is a globally prevalent disease and major cause of tooth loss in adults, which affects human health and quality of life. In recent decades, several strategies have been adopted to reconstruct periodontal tissues such as bone grafting, guided tissue regeneration, enamel matrix derivative, fibroblast growth factor, and platelet-derived growth factor (PDGF). However, pre-clinical and clinical studies revealed the restricted regeneration potential and unpredictable outcomes of these strategies, particularly in cementum and functional periodontal ligament regeneration [1]. Tissue engineering provides new strategies for preparing human tissues and treating organ defects. Periodontal tissue engineering can promote the formation of new periodontal attachment via stem cells or progenitor cells [2,3].

The most common strategy used for periodontal reconstruction is an implant scaffold material seeded with cells into the periodontal defect. Conventional tissue engineering procedures involve trypsin digestion to acquire seeding cells, which lose their original extracellular matrix components and cell-cell connections. To overcome these limitations, cell sheet technology was developed by Kwon et al. [4]. The cell sheet has also been used in periodontal tissue regeneration [5–7]. A previous study showed that dental follicle cell sheets (DFSCs) showed better biological properties and stronger capacity for ectopic periodontal tissues regeneration *in vitro* compared to the periodontal ligament cell sheet [8]. A study also showed that a combination of DFSCs and treated dentin matrix (TDM) formed dentin-pulp like tissues and cementum-periodontal complexes *in vivo* [9]. Thus, DFSCs may be an appropriate seed cell delivery strategy in periodontal complex regeneration.

In bone tissue engineering, synthetic bone materials including hydroxyapatite (HA), tricalcium phosphate (TCP), bioactive glass, ceramics, and various polymers are commonly used, but these materials lack osteogenic induction ability [10,11]. Numerous studies have used teeth as bone graft material for clinical and histological research [12,13]. The components of teeth, particularly dentin, are similar to those of bone, which consists of collagen (20%), hydroxyapatite (70%), and body fluid (10%) [14]. TDM is a dentin-based biomaterial, generated by sequential demineralization and shows good biocompatibility and bioactivity. TDM contains a large number of osteogenic/odontogenic-related proteins [15], which can induce the differentiation of dental follicle cells and regeneration of the cementum-periodontal ligament complex structure [9,16,17]. Studies showed that after implantation of the TDM, bone absorptive lacunae were observed on the implant surface in the tooth socket and TDM was integrated with the surrounding alveolar bone [18]. Thus, TDM may be useful as a bone graft material in regenerative medicine.

Periodontal tissue regeneration refers to the deposition of new cell-free cementum on the dentin surface or original cementum surface after periodontal treatment, and re-embedding of functional collagen fiber bundles between the teeth and alveolar bone to regenerate new attachment sites on diseased teeth and to achieve complete recovery of the periodontal tissue structure and function. In this study, allogeneic DFSCs and treated dentin matrix particles (TDMPs) were used to regenerate periodontal tissue. This study explored suitable, clinically viable seed cells, appropriate scaffold materials, and suitable delivery forms, to provide a theoretical and experimental basis for optimizing periodontal tissue regeneration strategies and future clinical applications.

2. Materials and methods

2.1. DFC culture and characterization

2.1.1. DFC isolation and subculture

The study was approved by Research Ethics Committee of West China Hospital of Stomatology (Project No. WCCSIRB-D-2015-144), while all patients signed an informed consent. DFCs were isolated and cultured as described previously [19]. Briefly, the tissue blocks were washed with phosphate-buffered saline (PBS) three times, and then incubated in α minimal essential medium (α-MEM; Hyclone, Logan, UT, USA) supplemented with 10% fetal bovine serum (Hyclone) in a humidified atmosphere at 37 °C and 5% CO_2. The cell culture medium was changed every 3 days. Cells from passages 3–5 were used in the experiments.

2.1.2. Colony-forming unit assays

A single-cell suspension was prepared, seeded at a density of 1000 cells per 100-mm dish (Corning, Inc., Corning, NY, USA) and maintained in the medium as described above. DFCs were fixed with 4% paraformaldehyde for 10 min, washed twice with PBS, and stained with Giemsa staining solution. Aggregates containing ≥50 cells were counted as colonies under a microscope (Olympus, Tokyo, Japan).

2.1.3. Multipotential differentiation

hDFCs were cultured in osteogenic medium or adipogenic medium as previously described [20]. The media were changed every 3 days for 3 weeks before the cells were stained with Alizarin Red (Sigma-Aldrich, St. Louis, MO, USA) or Oil red O (Sigma-Aldrich). For neurogenic differentiation, hDFCs were cultured in neurogenic medium for 2 h [17]. Next, the cells were fixed in 4% paraformaldehyde before they were immunocytochemically stained with anti-βIII-tubulin antibody (Millipore, Billerica, MA, USA). Nuclei were counterstained with 4′, 6-diamidino-2-phenylindole (Sigma-Aldrich).

2.1.4. *Immunofluorescence staining*

hDFCs were seeded at a density of 1×10^5 per well in a 6-well plate and incubated in a humidified atmosphere at 37 °C and 5% CO_2. The cells were then fixed with 4% paraformaldehyde for 10 min and washed twice with PBS before immunocytochemical staining with anti-vimentin (1:500, R&D Systems, Minneapolis, MN, USA), anti-Stro-1 (1:100, R&D Systems), and anti-Cytokeratin 14 (CK14, 1:500, R&D Systems) according to the manufacturer's instructions. Next, the cells were visualized with relevant Alexa Fluor® 488- or 555-conjugated secondary antibodies (Invitrogen, Carlsbad, CA, USA). The stained cells were observed under a fluorescent microscope (Olympus).

2.1.5. *Flow cytometric analysis*

For immunophenotype characterization, hDFCs were trypsinized, re-suspended, incubated with CD3-Fluorescein isothiocyanate (FITC) (1:100, BD Biosciences, San Jose, CA, USA), CD33-FITC (1:100, BD Biosciences), CD34-FITC (1:100, BD Biosciences), CD45-FITC (1:100, BD Biosciences), CD29-phycoerythrin (PE) (1:100, BD Biosciences), CD44-FITC (1:100, BD Biosciences), CD90-FITC (1:200, BD Biosciences), CD105-PE (1:200, BD Biosciences), and CD166-PE (1:100, BD Biosciences) for 1 h at 4 °C. Flow cytometry was performed on a BD Accuri™ C6 flow Cytometer (BD Biosciences).

2.2. *Cell sheet preparation and characterization*

2.2.1. *Cell sheet preparation*

A total of 1×10^5 hDFCs per well were seeded into a 6-well plate and cultured in a humidified atmosphere at 37 °C and 5% CO_2 until they reached confluence. Next, the medium was changed to α-MEM supplemented with 10% fetal bovine serum and 50 μg/mL ascorbic acid (Sigma-Aldrich). The medium was refreshed every three days for two weeks to form cell sheets. The hDFCs sheets (DFCSs) were re-seeded into a new 6-well plate and cultured in a humidified atmosphere at 37 °C and 5% CO_2 supplemented with α-MEM containing 10% fetal bovine serum.

2.2.2. *Histological examination*

hDFCSs were fixed in 4% paraformaldehyde before washing with PBS three times. The cell sheets were dehydrated using graded sucrose solutions (10%, 20%, and 30%) for 24 h each. The samples were frozen embed in optimal cutting temperature compound and stored at −80 °C until they were sectioned using a Leica CM1860 cryomicrotome (Leica Microsystems, Wetzlar, Germany). Sections (8 μm) were stained with hematoxylin and eosin (H&E) according to the manufacturers' instructions.

2.2.3. *Live/dead viability assay*

The hDFCSs and hDFCs were incubated with 4 mM ethidium homodimer-1 and 2 mM calcein-AM in PBS for 5 min (Weikaibioeng, Tianjing, China) according to the manufacturers' instructions. Images were acquired under a fluorescent microscope (Olympus).

2.2.4. *Immunohistochemical staining of hDFCSs*

Immunohistochemical staining of hDFCSs was performed using anti-fibronectin (1:200, Abcam, Cambridge, UK), anti-collagen I (Col I; 1:500, Abcam), and anti-osteopontin (OPN; 1:500, Abcam) according to the manufacturer's instructions. Images were acquired under a fluorescent microscope (Olympus).

2.2.5. *Real-time PCR analysis*

Total RNA was isolated from hDFCs and the hDFCSs with RNAiso Plus (TaKaRa Biotechnology, Shiga, Japan) according to the manufacturer's instructions. cDNA was synthesized using Thermo Scientific Revert Aid First Strand cDNA Synthesis Kit (Thermo Fisher Scientific, Waltham, MA, USA). Real-time PCR was conducted on a QuantStudio™ 6 Flex Real-Time PCR system (Thermo Fisher Scientific) using SYBR Premix Ex Taq (Perfect Real Time) (TaKaRa Biotechnology). Data were analyzed with QuantStudio™ Real-Time PCR software v1.2 (Thermo Fisher Scientific). The primers were synthesized by Sangon Biotech (Shanghai, China). The primer sequences are listed in Supplemental Table 1.

2.3. *Fabrication and characterization of humanTDMPs*

2.3.1. *Fabrication of TDMPs*

Twenty premolars were harvested from ten patients requiring removal of the premolars for clinical reasons at the West China Stomatology Hospital of Sichuan University with informed patient consent. Human TDM was prepared as described previously [9]. Next, the dentin matrix was frozen in liquid nitrogen for 5 min before grinding with a grinder (1200 rpm/min, 1 min, 3–5 times). The dentin matrix particles were treated three times with 17%, 10%, and 5% ethylene diamine tetra-acetic acid (Sigma-Aldrich) for 10 min. The obtained TDMP samples were freeze-dried for 8 h and then stored at −80 °C before Co^{60} radiation sterilization. Biphasic HA/TCP was provided by the National Engineering Research Center for Biomaterials of Sichuan University and served as control materials.

2.3.2. *Scanning electron microscopy*

TDMP and HA/β-TCP particles were observed by scanning electron microscopy (Inspect F, FEI, Eindhoven, The Netherlands).

2.3.3. *Particle size analysis*

Particle size of TDMP was analyzed with a laser diffractometer (HELOS/RODOS, Sympatec GmbH, Clausthal-Zellerfeld, Germany).

2.3.4. *Crystal phase analysis*

The phase structure of TDMP was characterized by X-ray diffraction (XRD, PANalytical EMPYREAN, Almelo, The Netherlands) using Cu Kα-radiation at a generator voltage of 40 kV and step scan of 0.0263° over a 2θ scan range of 20–80° according to a published protocol.

2.3.5. *X-ray photoelectron spectroscopy*

The chemical composition of TDMPs was characterized by X-ray photoelectron spectroscopy (XPS, KRATOS, XSAM 800) as previously described [21].

2.3.6. Surface functional groups analysis

The chemical properties of TDMPs were characterized by Fourier transform infra-red spectroscopy (Nicolet 6700; Thermo Fisher Scientific) as described previously [21].

2.3.7. Enzyme-linked immunosorbent assay (ELISA)

TDMPs were incubated for 1–13 days at a ratio of 1 g scaffold particles per 5 mL α-MEM at 37 °C. Next, the samples were filtered through a 0.22-μm filter. The resulting concentration of different growth factors was measured using ELISA kits (R&D Systems) for transforming growth factor (TGF-β), vascular endothelial growth factor (VEGF), bone morphogenetic protein-2 (BMP2), and platelet derived growth factor BB (PDGF-BB) according to the manufacturer's instructions.

2.4. Osteogenic effect of TDMP

2.4.1. Effect of TDMP extract on proliferation of bone marrow stromal cells (BMSCs)

BMSCs were isolated and cultured as described previously [22] in a humidified atmosphere at 37 °C and 5% CO_2. The medium was refreshed every 3 days. The TDMP extract and HA/β-TCP were incubated for 7 days at a ratio of 1 g scaffold particles per 5 mL α-MEM at 37 °C. Next, the extract supplemented with 10% fetal bovine serum was added to the wells. Cell Counting Kit-8 (CCK-8, Dojindo Molecular Technologies, Kumamoto, Japan) was used to evaluate cell proliferation according to the manufacturer's instructions.

2.4.2. Effect of TDMP extract on osteogenic differentiation of BMSCs

Passage 4 BMSCs were seeded into a 6-well plate at a density of 1×10^5/mL. The cells were then cultured with TDMP extract and HA/β-TCP extract supplemented with 10% fetal bovine serum for 7 days. The medium was refreshed every three days. The cells were collected for real-time PCR analysis as described above.

Total proteins were extracted using a RIPA Kit (KeyGEN, Nanjing, China), and total protein content was determined using bicinchoninic acid Protein Assay Kit (KeyGEN) according to the manufacturer's instructions. These samples were subjected to 12% sodium dodecyl sulfate-polyacrylamide gel electrophoresis and then transferred to a polyvinylidene fluoride membrane. The membranes were blocked in 5% fat-free dry milk and then incubated with primary antibodies including anti-OPN (1:1000, Abcam), anti-Col I (1:1000, Arigo, Hisinchu City, Taiwan), anti-runt-related transcription factor 2 (Runx2; 1:500, Santa Cruz Biotechnology, Dallas, TX, USA) and glyceraldehyde 3-phosphate dehydrogenase (GAPDH; 1:1000, Zen-bio, China) at 4 °C overnight. The membranes were incubated with appropriate horseradish-peroxidase-conjugated secondary antibodies before analysis by chemiluminescence using Immobilon™ Western Chemiluminescent HRP Substrate (Millipore) on an ImageQuant LAS 4000 min. (GE Healthcare Life Science, Little Chalfont, UK).

2.4.3. Preparation of rat calvarial bone defect

All animal experiments in this study were conducted in accordance with the Declaration of Helsinki under protocols reviewed and approved by the West China Hospital of Stomatology Institutional Review Board in Sichuan University (Project No. WCHSIRB-D-2014-141). A total of thirty-six 8-week-old Sprague-Dawley (SD) rats were used. A critical size bone defect of 5-mm diameter was created in the skull using a trephine. Three groups were divided: blank control, TDMP, and HA group. Each group contained 12 rats.

2.4.4. Radiograph analysis

The animals were sacrificed, and the samples were harvested at 2, 4, and 8 weeks. The specimens were fixed in 4% formalin solution for 24 h and washed under running water for another 24 h. Micro-computed tomography (CT) (SkyScan 1176 desktop X-ray micro-CT system, Skyscan, Bruker, Billerica, MA, USA) examination was conducted to assess new bone formation at the defect sites. The following parameters were set: 90 kV source voltage, 270 μA source current, and 1 mm aluminum filtration. These images were reconstructed as BITMAP files via SkyScan NRecon cone beam reconstruction software and bone volume/tissue volume (BV/TV) and trabecular number (Tb.N) were analyzed.

2.4.5. Histological analysis

The samples were decalcified in 10% ethylenediaminetetraacetic acid (pH 7.4) for 2 months, dehydrated with a graded series of ethanol, and embedded in paraffin wax. Next, 5-μm thick sections were prepared for H&E staining according to the manufacturer's recommended protocols.

2.5. Effect of TDMP extract on osteogenic differentiation of DFCSs

DFCSs were cultured in TDMP extract, HA/β-TCP extract, or growth medium in a humidified atmosphere at 37 °C and 5% CO_2 for 5 and 10 days.

2.5.1. Real-time PCR analysis

Real-time PCR was performed as described above to evaluate periodontal-related gene expression. The primer sequences are listed in Supplemental Table 1.

2.5.2. Western blotting

Western blotting was performed as described above. The following antibodies were used: fibronectin (1:500, Abcam), collagen III (1:500, Abcam), OPN (1:1000, Abcam), periodontal ligament-associated protein-1 (PLAP-1; 1:1000, Abcam), osterix (OSX; 1:1000, Abcam), alkaline phosphatase (ALP, 1:1000, Zen-bio, Research Triangle Park, NC, USA), Periostin (1:500, Santa Cruz), Runx2 (1:500, Santa Cruz), scleraxis (1:1000, Santa Cruz), cementum protein 23 (cp-23; 1:500, Santa Cruz), cementum attachment protein (CAP; 1:1000, Santa Cruz), collagen I (1:1000, Arigo), and GAPDH (1:1000, Zen-bio).

2.6. Effects of allogeneic TDM/DFCSs on periodontal bone regeneration

To further evaluate the potential of using TDM for periodontal regeneration, we prepared one-wall periodontal intrabony defects on beagle dogs.

2.6.1. *Culture of canine dental follicle cell sheets (cDFCSs)*

The tooth germ of first molars was collected after anesthesia from 2-month-old beagle dogs. Next, cDFCs were isolated, cultured, and cDFSCs harvested as described above for hDFCs and hDFCSs.

2.6.2. *Fabrication of canine TDMPs*

Canine TDMPs were prepared using a similar protocol as described above for human TDMPs.

2.6.3. *Prepare of one-wall periodontal intrabony defects*

All animal experiments in this study were conducted in accordance with protocols approved by the Ethics Committee of Sichuan University. The declaration of Helsinki under protocols reviewed and approved by the West China Hospital of Stomatology Institutional Review Board in Sichuan University (Project No. WCHSIRB-D-2014-141). One-wall periodontal intrabony defects were prepared as previously described [5,23]. Briefly, four male beagle dogs aged 1–5 years were used in this study. The first and third premolars in Beagle dog's bilateral mandibular were removed. Three months after tooth extraction, basic periodontal treatment was performed. Buccal and lingual mucoperiosteal flaps were elevated, and one-wall intrabony defects (5 × 4 mm) were prepared at the mesial side of the mandibular fourth premolars bilaterally using a high-speed handpiece. The periodontal ligament and cementum were removed with a diamond bur, and a groove was made to mark the surgical site (Fig. 6C). Six groups were randomly prepared: blank group, cDFCSs group, TDMP group, HA/β-TCP group, TDMP + cDFCSs group, and HA/β-TCP + cDFCSs group. The cDFCSs were placed close to the exposed root, gingival flaps were restored and sutured, and then the eugenol cement/iodoform periodontal pack (Dassoul, Xian, China) was placed. Soft diets were fed to the animals for one week.

2.6.4. *Imaging observation and measurement*

After 8 weeks, the animals were sacrificed under anesthesia. The mandibles were harvested and fixed using 4% paraformaldehyde for 7 days and washed under running water for 3 days. Next, the samples were scanned by micro-CT (SkyScan 1176 desktop X-ray micro-CT system). The following parameters were set: 90 kV source voltage, 270 μA source current, and 1 mm aluminum filtration. These images were reconstructed as BITMAP files with SkyScan NRecon cone beam reconstruction software. The region of interest was selected at the periodontal intrabony defects sites and new bone formation was measured and analyzed.

2.6.5. *Histology analysis*

Histology was performed using a similar protocol as described above. Image-Pro Plus 6.0 was used to measure long junctional epithelium height, connective tissue attachment height (CTA), cementum regeneration height (CR), cementum width, and periodontal ligament width.

2.7. *Statistical analysis*

All data are presented as the mean ± standard deviation (SD). One-way analysis of variance ($\alpha = 0.05$) was performed to compare more than two groups, and Student's t-test was used to compare two groups. Statistical significance was analyzed using SPSS 11.5 software (SPSS, Inc., Chicago, IL, USA). A $p < 0.05$ was considered to indicate a statistically significant difference.

3. Results

3.1. *Characterization of DFCs*

After subculture, DFCs exhibited a typical long spindle shape, similar to the fibroblast-like morphology (Fig. 1A), and formed colonies (Fig. 1B, C). Mineral nodes formed after osteogenic induction (Fig. 1D). Under adipogenic induction, lipid droplets were formed (Fig. 1E). Tubulin expression was detected after neural differentiation induction. DFCs were positive for the mesenchymal stem cell markers stro-1 (Fig. 1G) and vimentin (Fig. 1H), but negative for the epithelial cell marker CK-14 (Fig. 1I βIII-tubulin). In flow cytometry, DFCs were positive for mesenchymal stem cell markers such as CD29 (98.1%), CD44 (94.2%), CD90 (93.7%), CD105 (75.9%), and CD166 (94.5%), but negative for hematopoietic markers such as CD3 (0.027%), CD33 (0.112%), CD34 (0.012%), and CD14 (0.037%) (Fig. 1J).

3.2. *Characterization of DFCSs*

After 2 weeks of culture, DFCSs were formed (Fig. 2A). Microscopy analysis showed that DFCs were arranged in a specific direction, showing a tendency for multilayer growth (Fig. 2B). H&E staining showed that the DFCSs mainly formed a monolayer or multilayer with a rich extracellular matrix (Fig. 2D). When the DFCSs were reseeded into the culture dish for 4 days, DFCs migrated from the edge of the DFCSs (Fig. 2E). Dead cells were rarely observed after long-term culture of DFCSs (Fig. 2C, F).

Both DFCs and DFCSs were positive for extracellular matrix proteins such as fibronectin, COL-I, and OPN (Fig. 2G). Periodontal markers such as PLAP-1, periostin, and scleraxis were increased in DFCSs compared in DFCs, while the cementum markers cp-23 and CAP and osteogenesis markers Runx2, ALP, and OSX were down-regulated (Fig. 2H).

3.3. *Characterization of TDMP*

TDMP formed canary yellow particles based on visual observation (Fig. 3A). Dentinal tubules were exposed, and collagenous fibers were loosened for TDMP (Fig. 3B, C). The particle sizes of TDMP were as follows: D50: 348.682 μm, D90: 470.049 μm, average particle size: 337.107 μm (Fig. 3D). XRD revealed that the characteristic peak of TDMP was consistent with the standard HAp patterns (JCPDS 72-1243), indicating that the major inorganic constituent of TDMP was HA. The half-peak width of TDMP was higher than that of synthetic HA, indicating that the crystalline structure was lower in TDMP than in synthetic HA (Fig. 3E). Fourier transform-infrared analysis revealed the presence of organic groups such as carbonate and phosphate groups in TDMP but the absence of HA/β-TCP (Fig. 3F). XPS revealed the presence of oxygen, copper, magnesium, and sodium in addition to the basic chemical element of HA such

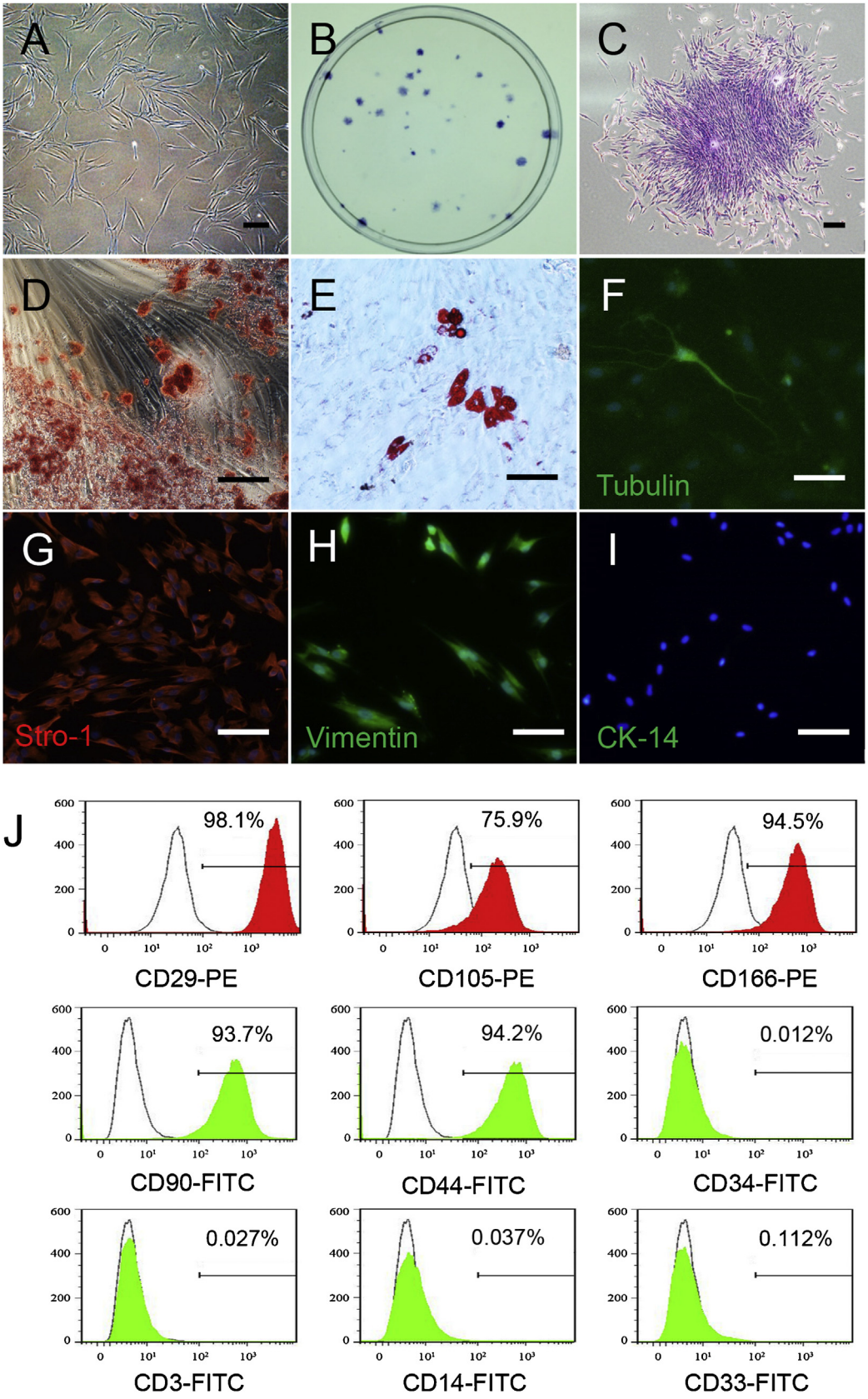

Fig. 1 – Evaluation of the biological characteristics of human dental follicular cells (DFCs). (A) Passage 3 human DFCs culture and Giemsa staining of CFU by visual (B) and microscopic (C) examination. Under appropriate induction conditions, mineralization nodes (D), lipid droplets (E), and neuronal-like cells (F) were formed in DFCs. DFCs were positive for stro-1 (G) and vimentin (H) but negative for CK-14 (I). Flow cytometric analysis revealed that DFCs were positive for CD29, CD44, CD90, CD105, and CD166 but negative for CD3, CD33, CD34, and CD14 (J).

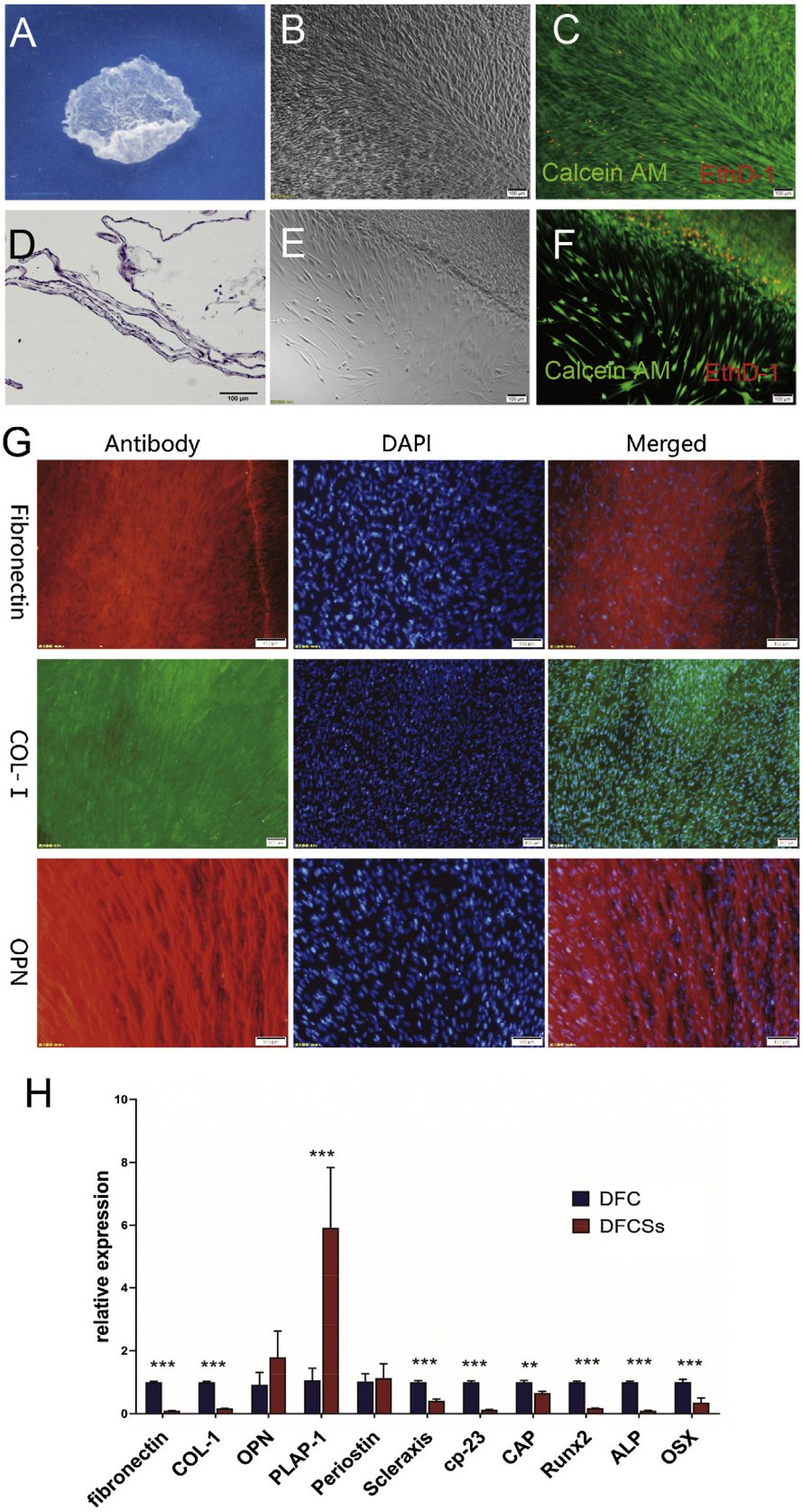

Fig. 2 – Characteristics of human dental follicle cells sheet. (A) DFCSs in the tissue culture plate after culture for 21 days *in vitro*. (B) Light microscope observation of DFCSs. (C) Live/dead staining. (D) H&E staining. (E, F) Living cells migrated from DFCSs. (G) DFCSs were positive for fibronectin, COL-I, and OPN. (H) Differences in gene expression between DFCs and DFCSs.

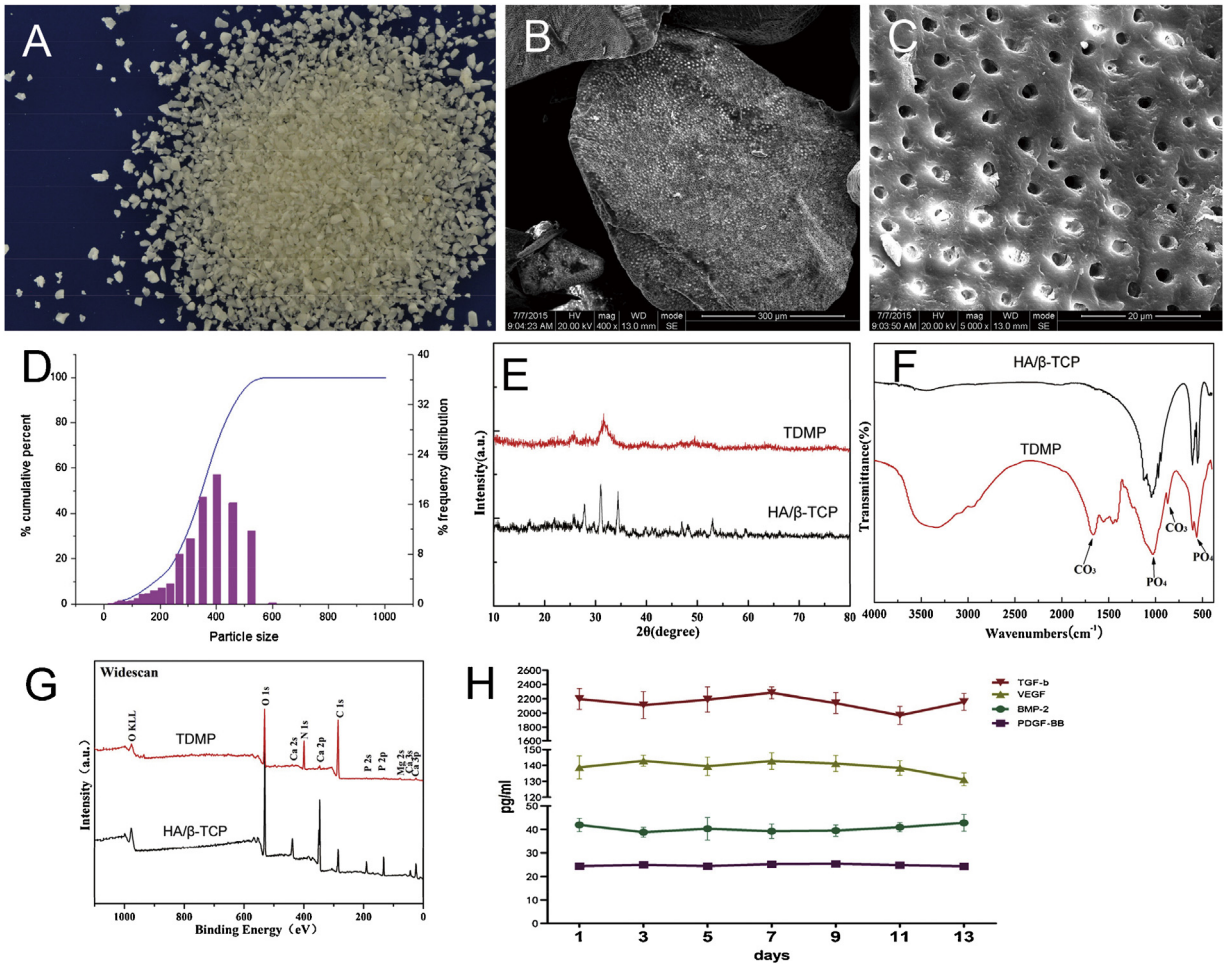

Fig. 3 – Characterization of hTDMP. TDMP evaluated by visual observation (A), scanning electron microscopy (B, C), particle size distribution (D), XRD (E), Fourier transform-infrared spectroscopy (F), X-ray photoelectron spectroscopy (G). ELISA results for TGF-β, VEGF, BMP-2, and PDGF-BB released by TDMP (H).

as calcium and phosphorus. TDMP contained more carbon and nitrogen, while HA/β-TCP had more calcium and phosphorus (Fig. 3G). The ELISA results showed constant release of TGF-β, VEGF, BMP2, and PDGF-BB from TDMP during days 1–13 (Fig. 3H).

3.4. *Osteogenic effect of TDMP*

3.4.1. *Effect of TDMP extract on proliferation and differentiation of BMSCs*

As shown in Fig. 4A, all three groups entered the logarithmic phase on day 2 and 6–7 days was the stagnate phase. Compared to the blank control and HA/β-TCP extract groups, TDMP promoted the proliferation of hBMSCs.

After culture in the TDMP extract for 7 days, real-time PCR showed that the expression of osteogenic markers such as OPN and Runx2 but not COL-I was increased in the TDMP group compared to in the other groups. Western blotting revealed an increase in COL-I and Runx2 but not OPN in the TDMP group compared to in the other groups (Fig. 4B).

3.4.2. *Bone regeneration of calvarial bone defect in SD rats*

Minimal new bone formation was observed at the edge of the defect area in the blank control group. After implantation for 2, 4, and 8 weeks, new bone formation was observed by X-ray in both the TDMP and HA/β-TCP groups (Fig. 4D). Microscopic structure parameter analysis revealed no significant difference in BV/TV and Tb.N between the TDMP and HA/β-TCP groups at week 8 (Fig. 4E) ($p > 0.05$), indicating that TDMP can induce new bone formation in calvarial bone defects.

3.4.3. *Histology analysis of calvarial bone defects in SD rats*

By H&E staining, stromal responsive fibrosis and reactive bone formation were observed at the edge of the calvarial bone defect in the TDMP and HA/β-TCP group. Unabsorbed particles were surrounded by fibrous connective tissue with microvessels. Defects in the blank control group were filled with fibrous connective tissue (Supplemental Fig. 1A). New bone formation was observed in the calvarial bone defect zone in both the TDMP and HA/β-TCP groups. Absorption was observed in the

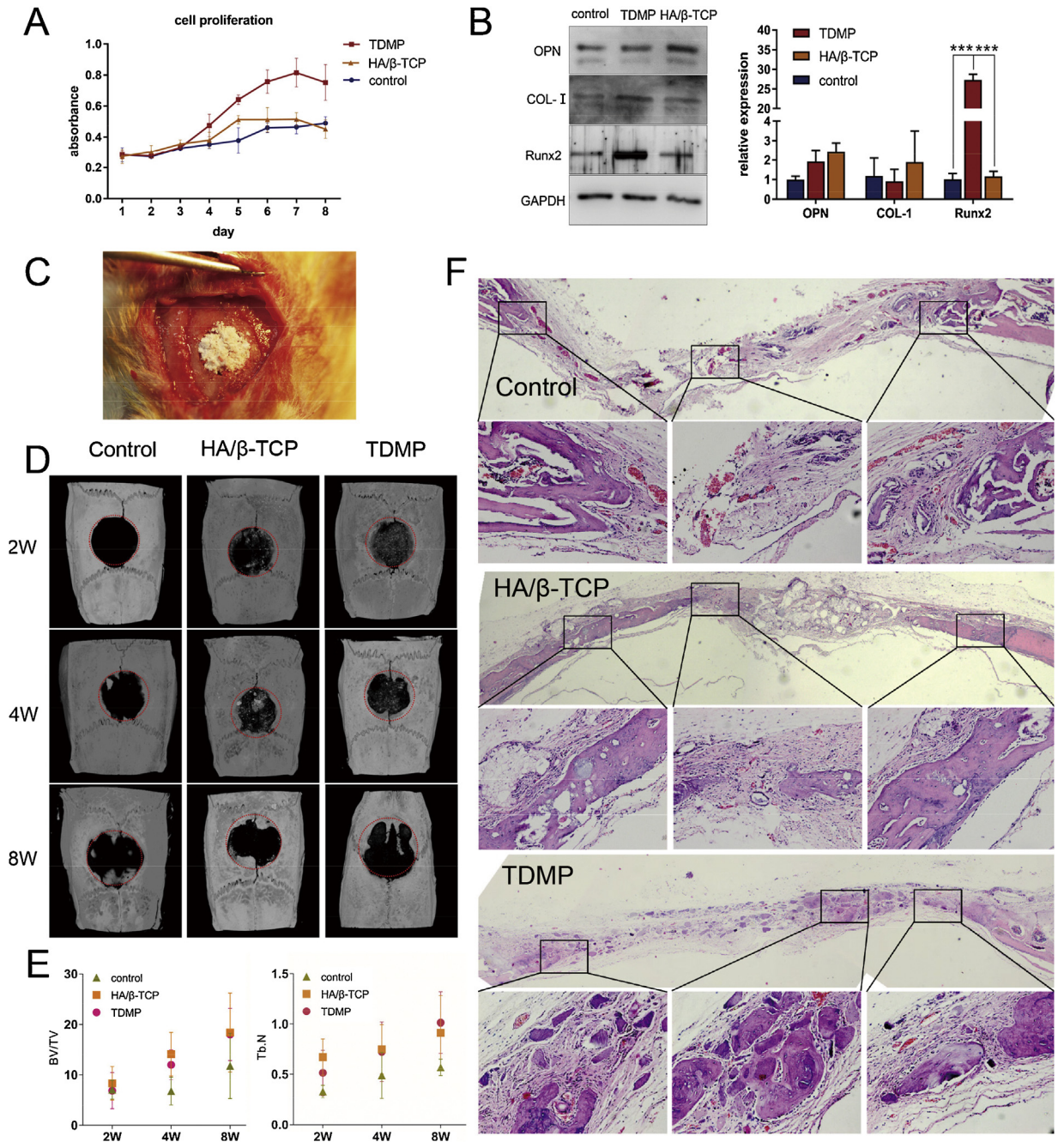

Fig. 4 – hTDMP as a biomaterial for bone regeneration. (A) Effect of hTDMP on hBMSC proliferation. (B) Effect of hTDMP on osteogenic differentiation of hBMSCs. (C) Prepare of calvarial bone defect in SD rats (Φ = 5 mm). (D) Micro-CT analysis after hTDMP implantation for 2, 4, and 8 weeks, BV/TV and Tb.N comparison (E). (F) H&E staining at 8 weeks after implantation.

HA/β-TCP group, but was not significant in the TDMP group (Supplemental Fig. 1B).

HA/β-TCP particles were observed after 8 weeks. The area of new bone formation was larger in the HA/β-TCP group at 8 weeks compared to at 4 weeks. HA/β-TCP particles were surrounded by osteoclasts and odontoblasts. Woven bone was gradually replaced by lamellar bone. Some TDMPs were not absorbed and were surrounded by fibrous connective tissue, while many particles were surrounded by new bone matrix. In contrast, new bone formation was observed at the edge of the defect area in the control group after 8 weeks post-implantation. The central region was filled with dense fibrous connective tissue (Fig. 4F).

3.5. *Effect of TDMP extract on differentiation of DFCSs*

Western blotting showed that the expression of extracellular matrix proteins such as fibronectin, COL-I, and OPN was increased in the TDMP groups compared to in the HA/β-TCP and control groups after 10 days of coculture. Western blotting and real-time PCR results showed that the expression of fibronectin was increased both at the mRNA and protein lev-

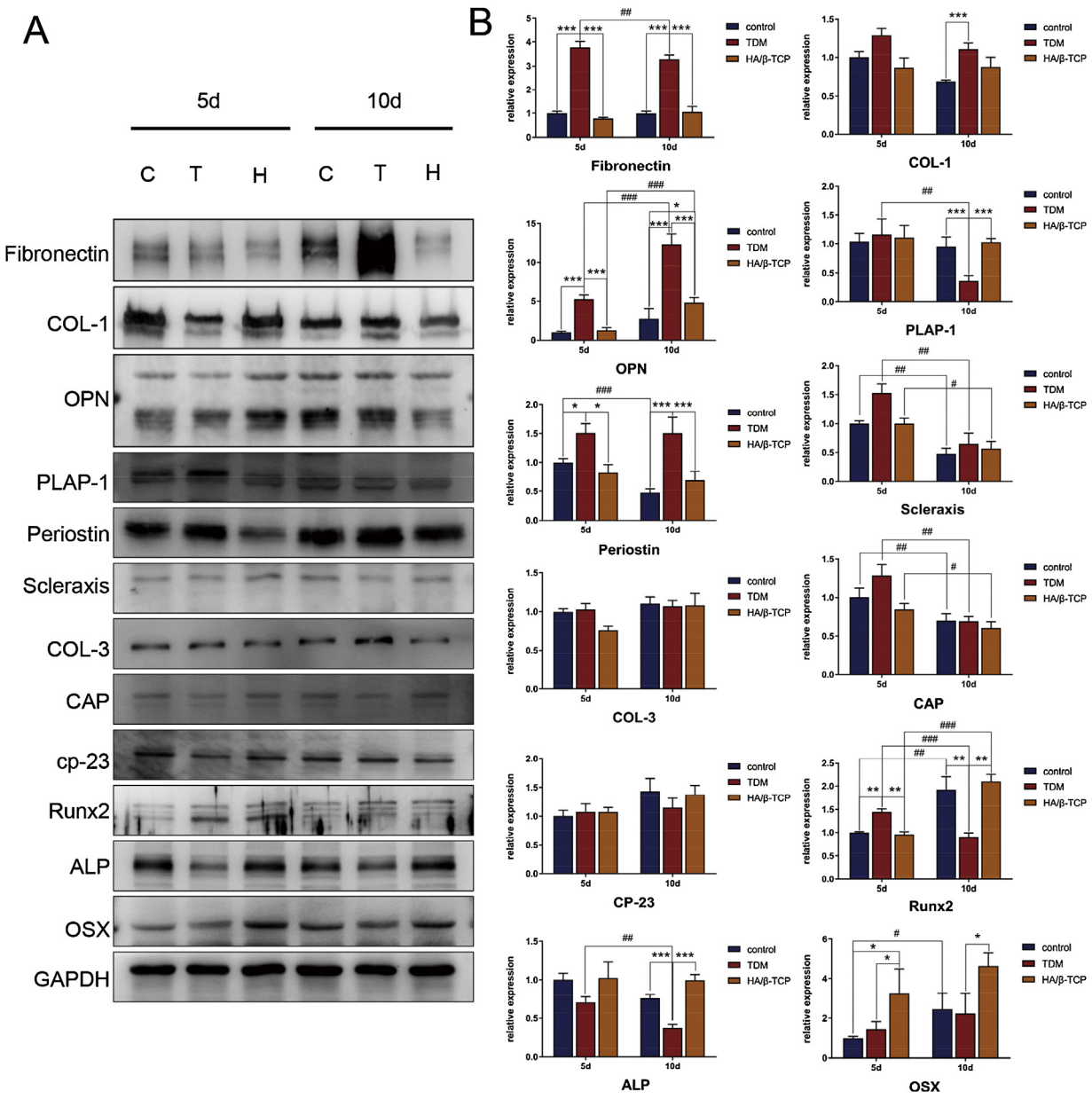

Fig. 5 – TDMP on DFCSs periodontal differentiation propensity. (A) Western blot analysis of proteins related to osteogenic and periodontal differentiation, C: control; T: TDMP; H: HA/β-TCP. (B) Real-time PCR analysis of markers related to osteogenic and periodontal differentiation.

els in the TDMP group compared to in the HA/β-TCP group. COL-I mRNA was significantly increased in the TDMP group compared to in the HA/β-TCP group on day 10, while protein expression was decreased on day 5 and increased on day 10. OPN was increased at the mRNA level but not at the protein level in the TDMP group compared to in the other groups (Fig. 5A, B).

The expression of periodontal-related markers was evaluated by real-time PCR and western blotting. The results showed that collagen III mRNA expression was not significantly different among groups, but significantly increased at the protein level. Scleraxis was not significantly differently expressed among different groups. However, PLAP-1 protein expression was increased in the TDMP group on day 5 but decreased at the mRNA level on day 10 compared to in the other groups (Fig. 5A, B). Cementum markers such as CAP and cp-23 were expressed in the three groups, the difference was not significant (Fig. 5A, B). Osteogenic-related markers such as Runx2, OSX, and ALP showed higher expression in the HA/β-TCP group than in the other groups (Fig. 5A, B).

3.6. *Effect of allogeneic TDM/DFCs sheets on periodontal bone regeneration in vivo*

3.6.1. *Characterization of canine TDMP and DFCSs*

Canine TDMP formed canary yellow particles were detected by visual observation (Fig. 6 A). Canine DFCSs formed after

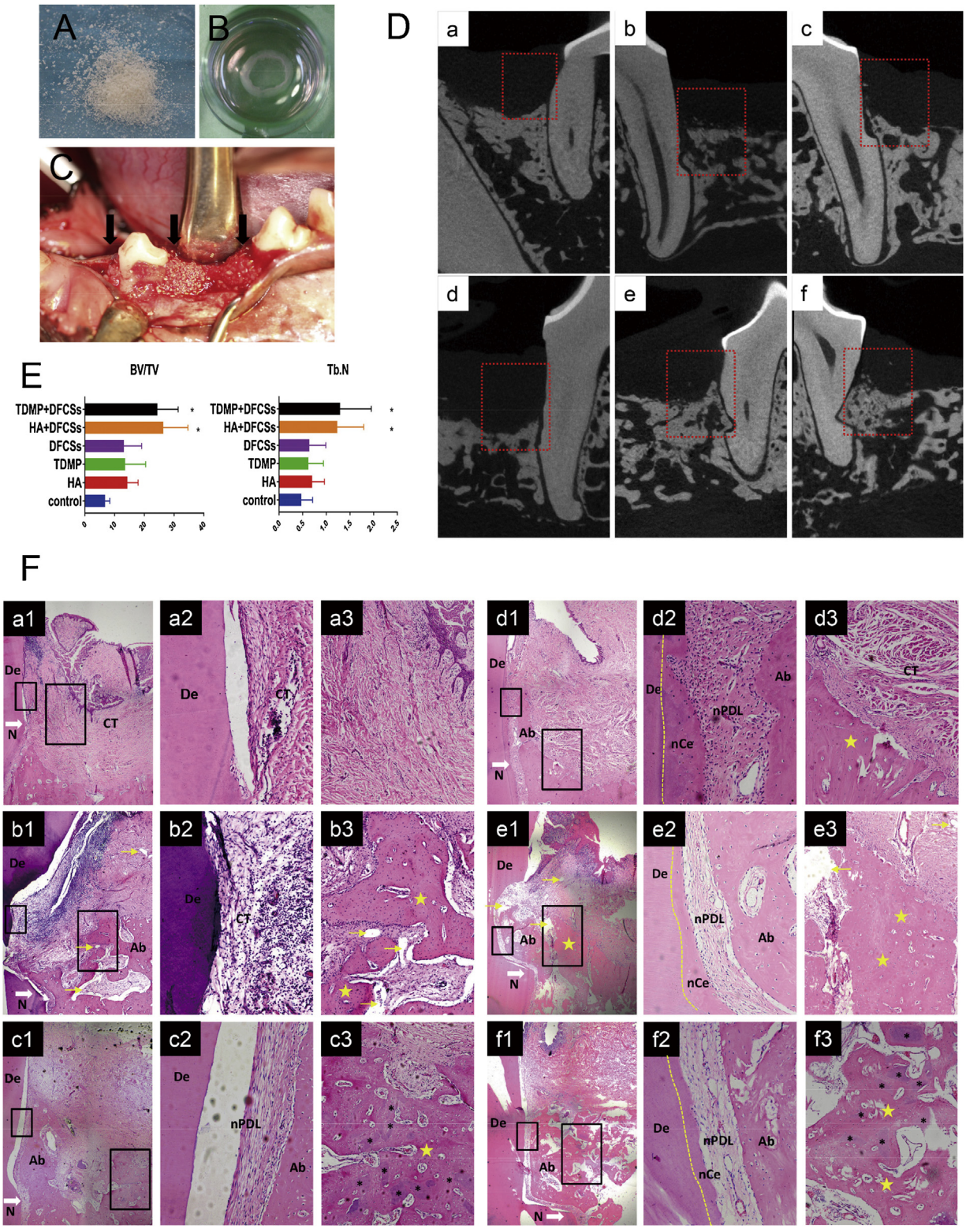

Fig. 6 – Allogeneic TDMP/DFCs sheets on periodontal bone regeneration. (A) Dog TDMP, (B) dog DFCs sheets were transplanted into the one-wall intrabony defect model in beagle (C) for 8 weeks. (D) μCT was conducted to analyze alveolar bone regeneration, a: blank control; b: HA/β-TCP groups; c: TDMP groups; d: DFCSs group; e: HA/β-TCP particles + DFCSs group; f: TDMP + DFCSs group. The red dashed box shows the area of the periodontal defect and "area of interest" in imaging analysis. (E) Periodontal regeneration was significant in both newly formed cementum, well-oriented PDL fibers, and amount of alveolar bone regeneration in the TDMP + DFCSs and HA/β-TCP + DFCSs groups. (a1–a3): blank group; (b1–b3): HA/β-TCP group; (c1–c3): TDMP group; (d1–d3): DFCSs group; (e1–e3): HA/β-TCP + DFCSs group; (f1–f3): TDMP + DFCSs group; the black box shows the enlarged area image as (a2–f2 and a3–f3). De: dentin; Ab: alveolar bone; N: root surface marker;

2 weeks of culture in medium containing ascorbic acid (Fig. 6B).

3.6.2. Micro-CT analysis

A small amount of new bone formation was detected at the bottom of the defect area in the blank control group at 8 weeks after implantation (Fig. 6D-a). TDMP and HA/β-TCP particles were not fully absorbed (Fig. 6D-b, c, e, f). More new bone formation was observed in the materials groups compared to in the groups without using materials. The bone tissue was denser and periodontal ligament space formed groups with DFCSs compared to in groups without cells (Fig. 6D-d, e, f).

3.6.3. Histological observations and measurement

Periodontal-like tissues were formed in groups with DFCSs and new bone formation was observed from the notch to the coronal side. Each group using DFCSs regenerated new periodontal tissue in the defect area. Different degrees of new bone formation were observed from the cut to the crown side. A layer of cementum-like mineralized tissue was observed on the dentin surface, with a bundle of periodontal ligament fiber embedded. One end was buried in newborn cementum-like tissue, while the other end was buried in new alveolar bone. The direction was perpendicular to the root surface, similar to the Sharpey's fiber, and the fibrous tissue was scattered in capillaries, which was similar to the natural periodontal tissue. In contrast, minimal periodontal tissue was regenerated in groups without DFCSs. The junctional epithelium moved to the root and dense fibrous tissue formation was observed near the natural dentin of TDMP and HA/β-TCP granule. The dentin surface showed no obvious new tooth bone structure under low magnification, and the periodontal gap was larger than that in the other groups. Little new bone formation was observed in the DFCSs alone group and was mainly detected in the periodontal region. The defect area was filled with dense fibrous connective tissue. In contrast, new bone formation was observed both in the TDMP group and TDMP + DFCSs group, and few TDMPs had not completely absorbed at 8 weeks after transplantation, while most were wrapped by new bone. New bone formation was observed both in the HA/β-TCP group and HA/β-TCP + DFCSs groups, a few of which were wrapped by new bone (Fig. 6F).

Histological measurement was performed to evaluate periodontal regeneration (Table 1). The length of the junctional epithelium in groups with DFCSs was significantly shorter than in the control group ($p < 0.05$). Additionally, the heights of cementum-like tissue in the HA/β-TCP, TDMP, DFCSs, HA + DFCSs, and TDMP + DFCSs group were significantly higher than that in the control group ($p < 0.05$). The thickness of cementum-like tissue and width of the periodontal-like structure in groups with DFCSs was significantly thicker than those without DFCSs ($p < 0.05$). In contrast to the HA/β-TCP + DFCSs group, the length of the junctional epithelium was shorter, while the height of cementum-like tissue was higher in the TDMP + DFCSs group ($p < 0.05$).

4. Discussion

The formation of new periodontal adhesion remains a major challenge in the field of periodontal tissue engineering, preventing complete recovery of periodontal tissue structure and function [1,24]. Because of the diversity of periodontal cells and uncontrolled regeneration environment, the transplanted cells must have multi-lineage differentiation capacity, and the scaffold materials are required to be multi-phase in accordance with the basic requirements of scaffold materials and even offer a related inductive microenvironment [25,26]. In this study, periodontal tissue was regenerated by combining DFCSs and TDMPs, indicating the potential of this strategy for periodontal tissue engineering.

Differences in animal models greatly affect the evaluation of tissue regeneration. Beagle dogs are widely used in experiments because their tooth size, periodontal tissue structure, and histopathology of periodontal disease are similar to those in humans [27]. The number of remaining walls is a key factor in the repair of periodontal intrabony defects. The buccal or lingual side wall of two-wall and three-wall periodontal intrabony defects can provide support to the soft tissue and form a self-supporting structure, creating a more stable structure environment for periodontal regeneration. Thus, the reparative potential of a one-wall periodontal intrabony defect is lower than that of a three-wall periodontal intrabony defect [28], which benefits the evaluation of regenerate therapeutic measurements [29]. Additionally, the occurrence of three-wall periodontal intrabony defect was less than 30% [30], and most of the defect was a combination of one-wall and two-wall. Thus, a one-wall periodontal intrabony defect model was created on beagle dogs to evaluate the efficiency of regenerative strategies in this study.

Previous studies showed that DFCs, as a type of mesenchymal stem cells, are candidates for regenerating toothroots [31]. In this study, the biological characteristics of DFCs were verified and their potential in periodontal tissue engineering was studied. Traditional periodontal tissue engineering involves loading of seed cells onto a scaffold material; however, the cell load is limited, and periodontal cells showed diversity and their local distribution range differed. Therefore, traditional tissue engineering methods cannot achieve higher density and accurate cell placement at the target location. The use of a cell sheet is an important strategy for overcoming these limitations. In this study, ascorbic acid was added to the culture to promote cell sheet formation. A cell sheet can form after 10 days of culture and can be harvested by mechanical methods [32,33]. The cell sheet is composed of a single-layer (multilayer in some area) of cells embedded in extracellular matrix, which

CT: connective tissue; nPDL: new periodontal ligament-like tissue; nCe: new cementum-like tissue; *: TDMP; yellow arrows: HA/β-TCP particles; yellow pentagram: new bone tissue; white arrows: the bottom of the root surface mark point; yellow dash line: the boundary between dentin and newly formed cementum-like tissue (For interpretation of the references to colour in this figure legend, the reader is referred to the web version of this article).

Table 1 – Histological measurement of periodontal regeneration after 8 weeks implantation (mean ± SD).

	Control	HA/β-TCP	TDMP	DFCSs	HA + DFCSs	TDM + DFCSs
LJE(mm)	1.15 ± 0.28	1.34 ± 0.31	1.04 ± 0.65	1.08 ± 0.23****	0.98 ± 0.23****	0.66 ± 0.12*,****,**,a
CTA(mm)	0.99 ± 0.49	0.85 ± 0.12	0.96 ± 0.15	0.90 ± 0.17	0.74 ± 0.34	0.72 ± 0.21**
CR(mm)	1.12 ± 0.24	2.32 ± 0.33*	2.27 ± 0.37*	2.20 ± 0.31*	2.13 ± 0.47*	2.79 ± 0.24*,**,***,a
cementum width(μm)	13.58 ± 6.62	17.39 ± 7.23	13.27 ± 8.58	34.19 ± 18.71*,****	35.46 ± 18.46*,****,***	35.26 ± 17.45*,**,***
periodontal width(μm)	201.10 ± 41.27	254.18 ± 183.07	226.99 ± 63.86	154.72 ± 58.07****,***	130.24 ± 46.82*,****,**	136.22 ± 46.48*,**,***

LJE: long junctional epithelium height; CAT: connective tissue attachment height; CR: cementum rengeneration height.

* vs. control $p < 0.05$.

** Vs. DFCSs $p < 0.05$.

*** vs. TDM $p < 0.05$.

**** vs. HA $p < 0.05$.

[a] TDM + DFCSs vs. HA + DFCSs, $p < 0.05$, n = 12 (In the measurement of the thickness of cementum-like tissue and new periodontal ligament-like tissue, 3 regions of the crown, middle, and root of the new periodontal ligament-like tissue structure from each slice were selected, and 3 measurements were made in each area).

constructs a "niche"-like structure, provides a platform for cell adhesion, and influences cell behaviors [34,35]. Additionally, extracellular matrix macromolecules and their specific domains play important roles in the wound healing process [36,37]. COL-I, fibronectin, and OPN are expressed in DFCSs, and facilitate the regeneration of bone tissue [38–40]. The expression of PLAP-1, periostin, scleraxis, cp-23, CAP, Runx2, ALP, and OSX in DFCSs indicated that the DFCSs can differentiate into multilineages. The expression of extracellular matrix and cementoblast genes in DFCSs was decreased, while PLAP-1, periostin, and scleraxis showed sustained expression and even elevation. This may be related to the longer culture of DFCSs than of DFCs. These results indicate that DFCs can differentiate into the periodontal cell lineage.

The natural establishment of adhesion between teeth and periodontal depends on cell proliferation at the site of injury [41,42]. This study found showed that the length of the junctional epithelium was shorter in the DFCSs group than in the other groups, which has two potential explanations. First, the DFCSs showed some viscosity and blood wetting, thereby creating a relatively stable structure on the root surface. Second, the stable structure of the wound can prevent epithelial migration to the root and produce long-binding epithelial healing, facilitating the attachment of other tissues to the root [1]. Although there were a few dead cells in DFCSs after the long period of culture, most DFCSs were alive. Subculture of DFCSs showed that many living cells migrated from the cell sheets, indicating that the cells migrate to adjacent damaged tissue and are involved in repairing tissue after implantation. Because DFCSs were placed on the root surface, DFCs preferentially occupy the root surface compared to autologous local cells, and thus settle on the root surface more quickly. Additionally, DFCs can secrete extracellular matrix to form bone-like tissue and periodontal-like tissue [31]. Therefore, we found that bone-like tissue in the three experimental groups using DFCSs was thicker than in the other three groups without DFCSs, resulting in a smaller periodontal gap and similar periodontal clearance of natural teeth. New cementum formation in the three groups without the use of DFCSs mainly depended on the migration of periodontal ligament cells of the defective root [24,43]. Thus, DFCSs play a vital role in periodontal tissue regeneration.

Periodontal tissue defects are caused by periodontitis and are often accompanied by various forms of alveolar bone tissue defects, which are beyond the repair ability of bone tissue. Therefore, bone graft materials are required to treat periodontal tissue defects. Compared to simple flap surgery, bone graft material filling can significantly improve the bone level and periodontal adhesion level and reduce the probing depth [44,45]. The most widely clinical used materials are calcium phosphate-based biomaterials and their composites [46–48]. In the current study, a characterization test showed that the basic component of TDM granules were low crystallinity hydroxyapatite, which contained a large number of organic groups such as CO_3^{2-} and a large number of inorganic constituents such as calcium, phosphorus, magnesium, copper, sodium, and other elements, indicating that its composition is far more complex than that of synthetic HA and closer to the composition of human bone [14,49]. The mechanical properties of implanted bone graft materials are relatively low because of the characteristics of the periodontal bone tissue defect; however, diversity in defect morphologies requires the plasticity of the transplanted material. As a result, we prepared the TDM as particles to facilitate their placement in the defect area, while the space between the particles facilitates the transport of nutrients, oxygen, and metabolites [50]. In histological observation of the calvarial bone defect model of SD rats and periodontal intrabony defect model of canine, TDMP formed new bone tissue at the defect while maintaining space, suggesting that material degradation can be regulated by changing the particle size, which was similar to the findings of Koga et al. [51]. The radiology and histology results showed that TDMP implantation did not lead to inflammation in local tissues, and TDMP extracts promoted the proliferation and differentiation of BMSCs *in vitro*, suggesting that TDMPs are biocompatible.

Currently, most materials used as bone tissue replacement materials do not contain growth factors or exhibit bone conduction other than bone induction ability, limiting their application in bone reconstruction [52]. In contrast, this study showed that TDMP can continuously release TGF-β, VEGF, BMP2, and PDGF-BB. The release of osteogenic components such as hormones, growth factors, and drugs using a local sustained release system with an osteoconductive biomaterial is an important strategy for designing bone graft materials [52].

in vitro experiments showed that TDMP extract promotes the proliferation and osteogenic differentiation of mesenchymal stem cells, which is consistent with the results of previous studies [16,17,53]. TDMP showed relatively stable release during days 1–13 and no obvious burst release was observed, which may be associated with the binding state of growth factors in the dentin matrix [54]. After implantation, growth factors may be further released during the degradation process, showing effective sustained release.

How to promote the early adhesion and osteogenic differentiation of osteoblast-related cells on the material surface is an important factor that must be considered in the design of bone graft materials. Interestingly, in the TDMP group, we found that TDM particles were visibly absorbed and wrapped by new bone matrix, while the exposed root surface was not visibly absorbed. This may be because the collagen fiber on the surface of TDMP was exposed after gradient demineralization, facilitating cell adhesion and proliferation, thus contributing to tissue regeneration and repair [55]. Because the tooth is easy to obtain, it is more economical than using other bone graft materials and can be obtained from autologous dental tissue to avoid biosafety problems [14]. Therefore, TDMP as a bone graft material showing local sustained release with both bone conduction and bone induction should be further developed for application. The effects of implant materials on seed cells are also important when selecting implant combinations. This study showed that TDMP extract treatment can increase the expression of fibronectin, collagen I, osteopontin, PLAP-1, periostin, and collagen III and inhibit the expression of ALP, OSX, and Runx2 in DFCSs, indicating that TDMP can influence the differentiation state of DFCSs [9]. Matching of scaffold materials with seed cells can affect regeneration [56]. From the perspective of developmental biology, mimicking the formation of periodontal tissue provides strategies for regeneration. According to the classical theory of the mesenchymal source, periodontal tissue formation in a microenvironment induced dental follicle differentiation. The microenvironment consists of dentin-matrix and epithelial cells [57]. Therefore, in this study, DFCSs were used to mimic dental follicle tissues and TDMPs were used to reconstruct the inductive microenvironment. The results showed that periodontal-like tissues were formed with a structure similar to that of the natural periodontal ligament gap.

New bone formed in the groups with materials and DFCSs was denser than in the other groups according to radiology and histology analysis. New bone formation was limited in the DFCSs alone group because of the poor mechanical properties of these cells, which cannot support the structure. Bone graft materials are required when DFCSs are used in periodontal regeneration [58]. The use of DFCSs improves the effectiveness of bone graft materials in bone defect repair, but the direct action of the cell sheets or effect of host cells recruited by DFCSs require further analysis [59].

5. Conclusions

In this study, TDMP showed ideal biocompatibility and suitable osteogenic inductivity, and successfully repaired critical-sized calvarial bone defects in SD rats. Thus, TDMP may be a feasible bone graft, and can serve as a substitute in clinical applications. The DFCSs may play a key role in periodontal tissue regeneration and can be used in an appropriate cell deliver strategy. Implantation of TDMPs combined with DFCSs into a one-wall periodontal intrabony defect resulted in periodontal tissue regeneration, verifying the potential for periodontal regeneration. Thus, the strategy should be further evaluated for clinical application. Additionally, the long-term periodontal regeneration effect requires verification.

Acknowledgements

This work was supported by the National Natural Science Foundation of China [grant numbers 81760197, 81660178, and 81700932] and Project of the Department of Science and Technology of Yunnan Province [grant number 2018FE001-317].

Appendix A. Supplementary data

Supplementary material related to this article can be found, in the online version, at doi:https://doi.org/10.1016/j.dental.2019.05.016.

REFERENCES

[1] Susin C, Wikesjo UME. Regenerative periodontal therapy: 30 years of lessons learned and unlearned. Periodontology 2000;2013(62):232–42.
[2] Fernandes G, Yang S. Application of platelet-rich plasma with stem cells in bone and periodontal tissue engineering. Bone Res 2016;4:16036.
[3] Monsarrat P, Vergnes JN, Nabet C, Sixou M, Snead ML, Planat-Benard V, et al. Concise review: mesenchymal stromal cells used for periodontal regeneration: a systematic review. Stem Cells Transl Med 2014;3(6):768–74.
[4] Kwon OH, Kikuchi A, Yamato M, Sakurai Y, Okano T. Rapid cell sheet detachment from poly(N-isopropylacrylamide)-grafted porous cell culture membranes. J Biomed Mater Res 2000;50(1):82–9.
[5] Tsumanuma Y, Iwata T, Washio K, Yoshida T, Yamada A, Takagi R, et al. Comparison of different tissue-derived stem cell sheets for periodontal regeneration in a canine 1-wall defect model. Biomaterials 2011;32(25):5819–25.
[6] Dan HX, Vaquette C, Fisher AG, Hamlet SM, Xiao Y, Hutmacher DW, et al. The influence of cellular source on periodontal regeneration using calcium phosphate coated polycaprolactone scaffold supported cell sheets. Biomaterials 2014;35(1):113–22.
[7] Ishikawa I, Iwata T, Washio K, Okano T, Nagasawa T, Iwasaki K, et al. Cell sheet engineering and other novel cell-based approaches to periodontal regeneration. Periodontology 2000;2009(51):220–38.
[8] Guo S, Guo W, Ding Y, Gong J, Zou Q, Xie D, et al. Comparative study of human dental follicle cell sheets and periodontal ligament cell sheets for periodontal tissue regeneration. Cell Transplant 2013;22(6):1061–73.
[9] Yang B, Chen G, Li J, Zou Q, Xie D, Chen Y, et al. Tooth root regeneration using dental follicle cell sheets in combination with a dentin matrix - based scaffold. Biomaterials 2012;33(8):2449–61.
[10] Giannoudis PV, Dinopoulos H, Tsiridis E. Bone substitutes: an update. Injury 2005;36(Suppl. (3)):S20–7.

[11] Bouler JM, Pilet P, Gauthier O, Verron E. Biphasic calcium phosphate ceramics for bone reconstruction: a review of biological response. Acta Biomater 2017;53:1–12.
[12] Catanzaro-Guimaraes SA, Catanzaro Guimaraes BP, Garcia RB, Alle N. Osteogenic potential of autogenic demineralized dentin implanted in bony defects in dogs. Int J Oral Maxillofac Surg 1986;15(2):160–9.
[13] Kim YK, Lee JH, Um IW, Cho WJ. Guided bone regeneration using demineralized dentin matrix: long-term follow-up. J Oral Maxillofac Surg 2016;74(3):e1–9, 515.
[14] Kim YK, Lee J, Um IW, Kim KW, Murata M, Akazawa T, et al. Tooth-derived bone graft material. J Korean Assoc Oral Maxillofac Surg 2013;39(3):103–11.
[15] Li J, Yang H, Lu Q, Chen D, Zhou M, Kuang Y, et al. Proteomics and N-glycoproteomics analysis of an extracellular matrix-based scaffold-human treated dentin matrix. J Tissue Eng Regen Med 2019 [Epub ahead of print].
[16] Guo WH, Gong K, Shi HG, Zhu GX, He Y, Ding BF, et al. Dental follicle cells and treated dentin matrix scaffold for tissue engineering the tooth root. Biomaterials 2012;33(5):1291–302.
[17] Li R, Guo W, Yang B, Guo L, Sheng L, Chen G, et al. Human treated dentin matrix as a natural scaffold for complete human dentin tissue regeneration. Biomaterials 2011;32(20):4525–38.
[18] Ji B, Sheng L, Chen G, Guo S, Xie L, Yang B, et al. The combination use of platelet-rich fibrin and treated dentin matrix for tooth root regeneration by cell homing. Tissue Eng Part A 2015;21(1–2):26–34.
[19] Yang H, Li J, Sun J, Guo W, Li H, Chen J, et al. Cells isolated from cryopreserved dental follicle display similar characteristics to cryopreserved dental follicle cells. Cryobiology 2017;78:47–55.
[20] Jiao L, Xie L, Yang B, Yu M, Jiang Z, Feng L, et al. Cryopreserved dentin matrix as a scaffold material for dentin-pulp tissue regeneration. Biomaterials 2014;35(18):4929–39.
[21] Li H, Sun J, Li J, Yang H, Luo X, Chen J, et al. Xenogeneic bio-root prompts the constructive process characterized by macrophage phenotype polarization in rodents and nonhuman primates. Adv Healthc Mater 2017;6(5):1601112.
[22] Luo S, Pei F, Zhang W, Guo W, Li R, He W, et al. Bone marrow mesenchymal stem cells combine with treated dentin matrix to build biological root. Sci Rep 2017;7:44635.
[23] Park S-H, Choi H, Han J-S, Park Y-B. Comparative study of decalcification versus nondecalcification for histological evaluation of one-wall periodontal intrabony defects in dogs. Microsc Res Tech 2015;78(1):94–104.
[24] Susin C, Fiorini T, Lee J, De Stefano JA, Dickinson DP, Wikesjo UM. Wound healing following surgical and regenerative periodontal therapy. Periodontology 2000 2015;68(1):83–98.
[25] Kim JH, Park CH, Perez RA, Lee HY, Jang JH, Lee HH, et al. Advanced biomatrix designs for regenerative therapy of periodontal tissues. J Dent Res 2014;93(12):1203–11.
[26] Babo PS, Cai X, Plachokova AS, Reis RL, Jansen J, Gomes ME, et al. Evaluation of a platelet lysate bilayered system for periodontal regeneration in a rat intrabony three-wall periodontal defect. J Tissue Eng Regen Med 2018;12(2):e1277–88.
[27] Weinberg MA, Bral M. Laboratory animal models in periodontology. J Clin Periodontol 1999;26(6):335–40.
[28] Kim CS, Choi SH, Chai JK, Cho KS, Moon IS, Wikesjo UME, et al. Periodontal repair in surgically created intrabony defects in dogs: influence of the number of bone walls on healing response. J Periodontol 2004;75(2):229–35.
[29] Kim CS, Choi SH, Cho KS, Chai JK, Wikesjo UME, Kim CK. Periodontal healing in one-wall intra-bony defects in dogs following implantation of autogenous bone or a coral-derived biomaterial. J Clin Periodontol 2005;32(6):583–9.
[30] Selvig KA, Kersten BG, Wikesjo UM. Surgical treatment of intrabony periodontal defects using expanded polytetrafluoroethylene barrier membranes: influence of defect configuration on healing response. J Periodontol 1993;64(8):730–3.
[31] Han C, Yang Z, Zhou W, Jin F, Song Y, Wang Y, et al. Periapical follicle stem cell: a promising candidate for cementum/periodontal ligament regeneration and bio-root engineering. Stem Cells Dev 2010;19(9):1405–15.
[32] Guo P, Zeng JJ, Zhou N. A novel experimental study on the fabrication and biological characteristics of canine bone marrow mesenchymal stem cells sheet using vitamin C. Scanning 2015;37(1):42–8.
[33] Wei F, Qu C, Song T, Ding G, Fan Z, Liu D, et al. Vitamin C treatment promotes mesenchymal stem cell sheet formation and tissue regeneration by elevating telomerase activity. J Cell Physiol 2012;227(9):3216–24.
[34] Gattazzo F, Urciuolo A, Bonaldo P. Extracellular matrix: a dynamic microenvironment for stem cell niche. Biochim Biophys Acta 2014;1840(8):2506–19.
[35] Watt FM, Huck WT. Role of the extracellular matrix in regulating stem cell fate. Nat Rev Mol Cell Biol 2013;14(8):467–73.
[36] Olczyk P, Mencner L, Komosinska-Vassev K. The role of the extracellular matrix components in cutaneous wound healing. Biomed Res Int 2014;2014:747584.
[37] Maquart FX, Monboisse JC. Extracellular matrix and wound healing. Pathol Biol 2014;62(2):91–5.
[38] Ferreira AM, Gentile P, Toumpaniari S, Ciardelli G, Birch MA. Impact of collagen/heparin multilayers for regulating bone cellular functions. ACS Appl Mater Interfaces 2016;8(44):29923–32.
[39] Agarwal R, Gonzalez-Garcia C, Torstrick B, Guldberg RE, Salmeron-Sanchez M, Garcia AJ. Simple coating with fibronectin fragment enhances stainless steel screw osseointegration in healthy and osteoporotic rats. Biomaterials 2015;63:137–45.
[40] Denhardt DT, Giachelli CM, Rittling SR. Role of osteopontin in cellular signaling and toxicant injury. Annu Rev Pharmacol Toxicol 2001;41:723–49.
[41] Melcher AH. On the repair potential of periodontal tissues. J Periodontol 1976;47(5):256–60.
[42] Melcher AH, McCulloch CA, Cheong T, Nemeth E, Shiga A. Cells from bone synthesize cementum-like and bone-like tissue in vitro and may migrate into periodontal ligament in vivo. J Periodontal Res 1987;22(3):246–7.
[43] Wolf M, Lossdorfer S, Abuduwali N, Meyer R, Kebir S, Gotz W, et al. In vivo differentiation of human periodontal ligament cells leads to formation of dental hard tissue. J Orofac Orthop 2013;74(6):494–505.
[44] Stein JM, Fickl S, Yekta SS, Hoischen U, Ocklenburg C, Smeets R. Clinical evaluation of a biphasic calcium composite grafting material in the treatment of human periodontal intrabony defects: a 12-month randomized controlled clinical trial. J Periodontol 2009;80(11):1774–82.
[45] Sculean A, Nikolidakis D, Nikou G, Ivanovic A, Chapple IL, Stavropoulos A. Biomaterials for promoting periodontal regeneration in human intrabony defects: a systematic review. Periodontol 2000 2015;68(1):182–216.
[46] Bhatt RA, Rozental TD. Bone graft substitutes. Hand Clin 2012;28(4):457–68.
[47] Hasan A, Byambaa B, Morshed M, Cheikh MI, Shakoor RA, Mustafy T, et al. Advances in osteobiologic materials for bone substitutes. J Tissue Eng Regen Med 2018;12(6):1448–68.
[48] Campana V, Milano G, Pagano E, Barba M, Cicione C, Salonna G, et al. Bone substitutes in orthopaedic surgery: from basic science to clinical practice. J Mater Sci Mater Med 2014;25(10):2445–61.

[49] Kim YK, Kim SG, Oh JS, Jin SC, Son JS, Kim SY, et al. Analysis of the inorganic component of autogenous tooth bone graft material. J Nanosci Nanotechnol 2011;11(8):7442–5.
[50] Aloy-Prosper A, Maestre-Ferrin L, Penarrocha-Oltra D, Penarrocha-Diago M. Bone regeneration using particulate grafts: an update. Med Oral Patol Oral Cir Bucal 2011;16(2):e210–4.
[51] Koga T, Minamizato T, Kawai Y, Miura K, Nakatani TIY, Sumita Y, et al. Bone regeneration using dentin matrix depends on the degree of demineralization and particle size. PLoS One 2016;11(1):e0147235.
[52] Martin V, Bettencourt A. Bone regeneration: biomaterials as local delivery systems with improved osteoinductive properties. Mat Sci Eng C Mater Biol Appl 2018;82:363–71.
[53] Widbiller M, Eidt A, Lindner SR, Hiller KA, Schweikl H, Buchalla W, et al. Dentine matrix proteins: isolation and effects on human pulp cells. Int Endod J 2018;51(Suppl. (4)):e278–90.
[54] Aubeux D, Beck L, Weiss P, Guicheux J, Enkel B, Perez F, et al. Assessment and quantification of noncollagenic matrix proteins released from human dentin powder incorporated into a silated hydroxypropylmethylcellulose biomedical hydrogel. J Endod 2016;42(9):1371–6.
[55] Kretlow JD, Mikos AG. 2007 AIChE Alpha Chi Sigma Award: from material to tissue: biomaterial development, scaffold fabrication, and tissue engineering. AIChE J 2008;54(12):3048–67.
[56] Chen G, Chen J, Yang B, Li L, Luo X, Zhang X, et al. Combination of aligned PLGA/Gelatin electrospun sheets, native dental pulp extracellular matrix and treated dentin matrix as substrates for tooth root regeneration. Biomaterials 2015;52:56–70.
[57] Yamamoto T, Yamamoto T, Yamada T, Hasegawa T, Hongo H, Oda K, et al. Hertwig's epithelial root sheath cell behavior during initial acellular cementogenesis in rat molars. Histochem Cell Biol 2014;142(5):489–96.
[58] Chen FM, Sun HH, Lu H, Yu Q. Stem cell-delivery therapeutics for periodontal tissue regeneration. Biomaterials 2012;33(27):6320–44.
[59] Yagi H, Soto-Gutierrez A, Parekkadan B, Kitagawa Y, Tompkins RG, Kobayashi N, et al. Mesenchymal stem cells: mechanisms of immunomodulation and homing. Cell Transplant 2010;19(6):667–79.